Weierstraß-Institut
für Angewandte Analysis und Stochastik

im Forschungsverbund Berlin e.V.

Preprint ISSN 0946 – 8633

Instabilities of stationary states in lasers with long-delay optical feedback.

Serhiy Yanchuk [1 2 3], Matthias Wolfrum[1]

submitted: 3. September 2004

[1] Weierstrass Institute
for Applied Analysis
and Stochastics
Mohrenstraße 39
D – 10117 Berlin
Germany
E-Mail: yanchuk@wias-berlin.de
wolfrum@wias-berlin.de

[2] Humboldt-University of Berlin
Institute of Mathematics
Unter den Linden 6
D – 10099 Berlin
Germany

[3] National Academy of Sciences of Ukraine
Institute of Mathematics
Tereshchenkivska 3
01060 Kiev, Ukraine

No. 962
Berlin 2004

2000 *Mathematics Subject Classification.* 34K60 34K20 34K26.

Key words and phrases. Lang-Kobayashi system, laser with feedback, external cavity mode, singularly perturbed delay-differential equation, stability.

This work was supported by DFG (Sonderforschungsbereich 555 "Komplexe nichtlineare Prozesse").

Edited by
Weierstraß-Institut für Angewandte Analysis und Stochastik (WIAS)
Mohrenstraße 39
10117 Berlin
Germany

Fax:	+ 49 30 2044975
E-Mail:	preprint@wias-berlin.de
World Wide Web:	http://www.wias-berlin.de/

Abstract

We study the Lang-Kobayashi model in the long-delay limit, focussing our attention on the stability properties of external cavity modes (ECMs) of this system. We show that ECMs can display different types of instabilities: strong instabilities and weak modulational-type instability. We explain the origin of these instabilities and show how they affect the complicated dynamics of the Lang-Kobayashi model.

1 Introduction

In this paper we study the dynamics of semiconductor lasers with optical feedback. This problem is of great practical importance since many optoelectronic systems contain semiconductor lasers as elements due to their small size and high efficiency.

The well-known Lang-Kobayashi (LK) model, which is still "simple enough" for detailed analytic investigations, has appeared [12] to be "complicated enough" to describe qualitatively many nonlinear phenomena, which occur in semiconductor lasers with feedback. The feedback injection is taken into account in this rate equation model via the delayed electric field amplitude. This leads to complicated dynamics which depend strongly on a few experimentally accessible parameters such as round-trip time in the external cavity and feedback strength.

In dimensionless form the LK system can be written as follows [17, 19, 1, 14]

$$\begin{aligned} E' &= (1+i\alpha)NE + \eta e^{-i\varphi}E(t-\tau), \\ N' &= \varepsilon[J - N - (2N+1)|E|^2]. \end{aligned} \tag{1}$$

This equation describes the evolution of the complex electric field $E(t)$ and excess carrier density $N(t)$. J is an excess pump current, τ is the external cavity round trip time measured in the units of the photon lifetime, η and φ are the feedback strength and round-trip phase-shift, respectively.

The model has been shown to describe many dynamical regimes of the laser, which are observed in experiments, cf. [8]. Concerning the limitations of the model and its derivation, we refer the reader to papers [9, 10, 14, 12, 17, 19] and references therein.

Periodic solutions of (1) of the form $E(t) = ae^{i\omega t}$, $N(t) = N = \text{const}$ are usually called external cavity modes (ECM). They are invariant with respect to the phase-shift symmetry $(E, N) \to (Ee^{i\psi}, N)$. ECM solutions correspond to stationary lasing states and are the starting point for the development of different dynamical regimes [4]. Even for large delay, the coexistence of stable ECMs and a chaotic regime was reported [3] numerically as well as experimentally. The complexity of the dynamics in the LK model develops with increasing delay τ, where most of the ECMs become unstable. In Sec. 2, we recall some known facts about ECMs and introduce a suitable parametrization.

Secs. 3 and 4 provide a new approach to the stability of ECMs. In particular, we show that the antimodes as well as modes with positive N are strongly unstable with a relaxation-type instability. The modes with negative N can exhibit modulational-type instability, which is a feature of spatially extended systems [15]. This observation is in agreement with the results of [6] about a connection between spatial and delayed systems.

As it was suggested in [4], ECMs can be considered as primary objects to create instability. Namely, they create another set of regular solutions, which form a ßkeletonöf the chaotic set. In more details we address this issue in Sec. 6.

Finally, Sec. 6 presents two examples, where properties of ECMs can give an additional insight on the properties of hyperchaotic pulsations in LK model.

2 Parametrization of the external cavity modes

In this section, we recall some important facts about the representation of ECMs of the Lang-Kobayashi system. We introduce a parameter along the family of ECMs, which then is used to classify different ECMs depending on their stability properties. We also obtain a probability distribution of ECMs, which holds asymptotically for large τ.

The equation for ECMs can be obtained by substituting $E(t) = ae^{i\omega t}, N(t) = N = \text{const}$ into (1), cf. [13, 17, 16, 19]:

$$\begin{aligned} N &= -\eta\cos(\varphi + \omega\tau), \\ \omega - \alpha N &= -\eta\sin(\varphi + \omega\tau), \\ a^2 &= (J - N)/(2N + 1). \end{aligned} \tag{2}$$

It is easy to see, that all ECMs satisfy the relation

$$N^2 + (\omega - \alpha N)^2 = \eta^2. \tag{3}$$

Geometrically, this is an ellipse in (ω, N) coordinates, cf. Fig 1. Let us denote $\theta := \varphi + \omega\tau$. Then θ can be considered as a parameter along the ellipse (3), such that $N = -\eta\cos\theta$ and $\omega - \alpha N = -\eta\sin\theta$. Positions of individual ECMs on the ellipse are given by solutions to the transcendental equation

$$\eta\tau(\sin\theta + \alpha\cos\theta) = \varphi - \theta. \tag{4}$$

The number of ECMs increases as $\eta\tau$ increases and can be estimated as $K = 2\tau\eta\sqrt{1 + \alpha^2}$, cf. [13]. For large τ, they become densely placed over the ellipse (3). The position θ of an individual ECM can be moved along the ellipse by varying the round-trip phase φ, keeping the other parameters fixed. Therefore, it is more convenient to investigate properties of

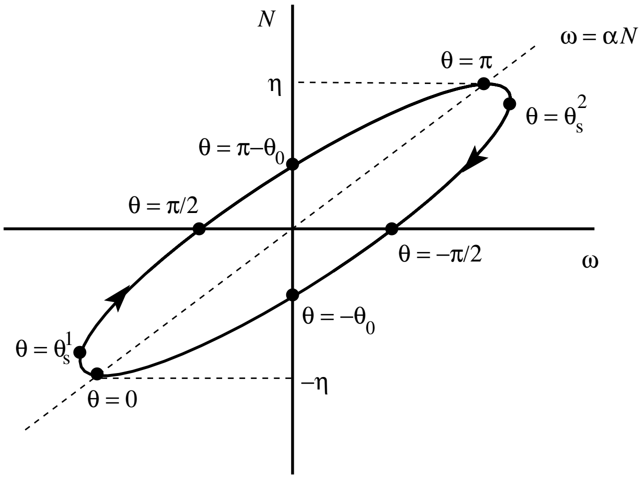

Figure 1: Representation of ECMs in (ω, N) coordinates. Parametrization by θ. The arrow indicates direction of the increasing of θ.

ECMs as a function of their position θ on the ellipse, rather then solving (4) for each particular parameter choice.

The value $\theta = 0$ corresponds to the maximum gain mode with $N = -\eta$ and $\omega = -\alpha\eta$.

With increasing η or τ, additional solutions appear in pairs at

$$\theta_s^1 := \arctan\frac{1}{\alpha} + \arcsin\frac{1}{\eta\tau\sqrt{1+\alpha^2}} \approx \arctan\frac{1}{\alpha}$$

and

$$\theta_s^2 = \arctan\frac{1}{\alpha} + \pi - \arcsin\frac{1}{\eta\tau\sqrt{1+\alpha^2}} \approx \arctan\frac{1}{\alpha} + \pi.$$

The ECMs with $\theta_s^1 < \theta < \theta_s^2$ are called antimodes [13, 3], while the others are modes. The antimodes have been shown [13] to be unstable with positive real eigenvalue.

It was also pointed out experimentally and numerically, that a laser diode with a weak to moderate optical feedback predominantly operates on the ECM with lowest linewidth, i.e. $\omega = 0$ and $\theta = -\theta_0 := -\arctan\alpha$, cf. [13] and references therein. For convenience, we summarize known types of ECMs in Table 1.

With the introduced parameter θ, one can visualize characteristics of the ECMs using the following expressions

$$\begin{aligned}
\tau(\theta) &= \frac{\varphi - \theta}{\eta(\alpha\cos\theta + \sin\theta)}, \\
N(\theta) &= -\eta\cos\theta, \qquad (5)\\
\omega(\theta) &= -\eta(\alpha\cos\theta + \sin\theta),
\end{aligned}$$

$\theta = 0$	maximum gain mode, $N = -\eta$, $\omega = -\alpha\eta$
$\theta_s^2 < \theta < \theta_s^1 + 2\pi$ $\theta = -\pi/2$ $\theta = -\theta_0$	modes $N = 0$, $\omega = \eta$ zero linewidth mode, $N = -N_0$, $\omega = 0$
$\theta_s^1 < \theta < \theta_s^2$ $\theta = \pi/2$ $\theta = \pi - \theta_0$	antimodes $N = 0$, $\omega = -\eta$ $N = N_0$, $\omega = 0$
$\theta = \pi$	$N = \eta$, $\omega = \alpha\eta$

Table 1: Known classification of ECMs.

which follow directly from (2). As an example, we plot in Fig. 2 frequency ω of ECMs versus τ using parametric plot of $\tau(\theta)$ and $\omega(\theta)$ with the free parameter θ.

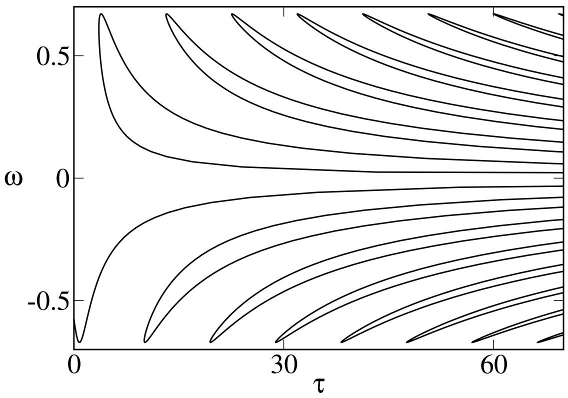

Figure 2: Frequencies of the ECMs versus delay. $\alpha = 2$, $\varphi = 1$, $\eta = 0.3$.

For large delay it is meaningful to speak about the distribution density of modes as a function of θ. In order to obtain this density, we consider equation (4) and rewrite it in the following form

$$-\eta\sqrt{1+\alpha^2}\sin(\theta + \theta_0) = \frac{\theta - \varphi}{\tau}. \tag{6}$$

The roots of (6) are given as the intersection points of the linear function at the right hand side and the sine function at the left hand side. Let us choose a large interval $\Delta\theta$ such that $1 \ll \Delta\theta \ll \tau$. Then the increment of the linear function is $dy = \Delta\theta/\tau$. On this interval, there are $dK \approx \Delta\theta/\pi$ intersection points. The element $d\theta$, containing the intersection points, is related to dy as $2dy = \eta\sqrt{1+\alpha^2}|\cos(\theta + \theta_0)|d\theta$. Here we take into account that there are two intersections per period. We get

$$2dy = 2\frac{\Delta\theta}{\tau} = 2\frac{\pi dK}{\tau} = \eta\sqrt{1+\alpha^2}|\cos(\theta + \theta_0)|d\theta$$

and hence

$$\rho(\theta) = \frac{dK}{d\theta} = \frac{\eta\tau\sqrt{1+\alpha^2}}{2\pi}|\cos(\theta + \theta_0)| \tag{7}$$

gives the distribution of ECMs along the ellipse (3).

Function (7) shows that the density of ECMs for large delay is not uniform and has maximum at the zero linewidth modes with $\theta = -\theta_0$ and $\theta = \pi - \theta_0$.

3 Stability of ECMs: numerical approach

In this section we perform numerically a stability analysis of different ECMs, using the software DDE-biftool software [5]. We fix $\tau = 100$, $\alpha = 2$, $\varepsilon = 0.03$ and $\varphi = 1.0$. For these parameters we have found 43 different ECMs.

Local stability of each ECM is determined by the set of eigenvalues of the linearized problem. Since the LK system (1) is infinite-dimensional due to the delay term, there is an infinite number of such eigenvalues. Eigenvalues with largest real parts play the decisive role for the stability. In the case when all eigenvalues have negative real parts, ECM is stable. On the other hand, it is unstable provided at least one eigenvalue has positive real part.

With DDE-biftool, we were able to compute the eigenvalues with the largest real parts for each ECM for a given set of parameters. We have found that they typically appear in four different configurations, shown in Fig. 3.

Fig. 3(a) represents the properties of the maximum gain mode, which appears to be stable for the given parameter values. We observe, that the characteristic roots in Fig. 3(a) are arranged in two branches.

The presence of such branches is a common feature of systems with large delay [20]. In particular, we will see in the next sections that the eigenvalues on these branches are related to some discrete mapping, which can be obtained in the limit of infinite delay.

One of the branches passes through the origin and contains the zero eigenvalue. This eigenvalue appears for all ECMs and exists because of the phase-shift invariance of the LK system. Therefore it does not influence the stability of the ECM. We will refer to this branch of eigenvalues, containing zero, as the *critical branch*. The imaginary parts of eigenvalues on the critical branch are approximately $\pm i\frac{2\pi}{\tau}, \pm i2\frac{2\pi}{\tau}, \pm i3\frac{2\pi}{\tau}, \ldots$. This fact can be confirmed by careful inspection of Fig. 3 and also will be proved analytically for the general case in Sec. 4. Hence, the leading eigenvalues, i.e. those, which are closest to the imaginary axis, have their imaginary parts close to $\pm i\frac{2\pi}{\tau}$. As a result, orbits in the vicinity of a stable ECM are attracted to it exhibiting periodic pulsations with the period close to τ, cf. Fig. 3(a).

Fig. 3(b) shows properties of the ECMs which are located between the maximum gain mode and the zero linewidth mode, i.e. $-\pi/2 < \theta < 0$. Now the critical branch has different curvature and contains eigenvalues with positive real parts.

This instability is similar to the modulational instability observed in spatially-extended systems [15]. The connection between delay systems and spatially extended systems was already studied in [6]. There, the authors pointed out that, especially for large delay, when

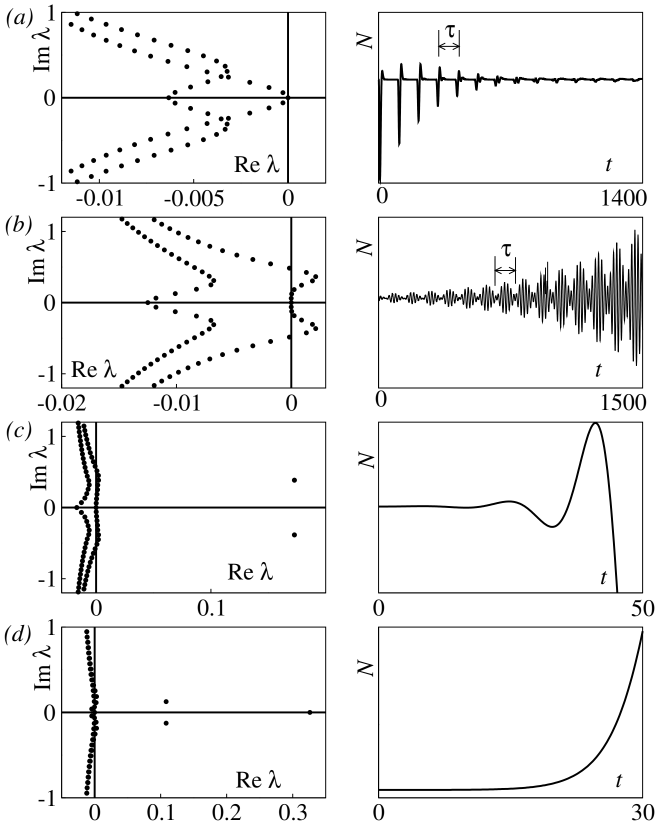

Figure 3: Local stability of ECMs for different typical cases. The left panel shows eigenvalues with the largest real parts and the right panel shows the behavior of an orbit, which starts in the vicinity of a given ECM. Parameter values: *(a)*: $\theta \approx 0$ (maximum gain mode), *(b)*: $\theta \approx 1.8\pi$, *(c)*: $\theta \approx 1.3\pi$, *(d)*: $\theta = 0.99\pi$ (antimode). Other parameters: $\tau = 100$, $\varphi = 1.0$, $\varepsilon = 0.03$, $J = 1$, $\eta = 0.3$.

the boundary conditions between connecting delay units play no significant role, delayed systems can be interpreted in terms of a suitable spatiotemporal dynamics. Likewise, the large delay is essential for the modulational-type instability which we observed here: one can speak about branches of eigenvalues and, therefore, about the modulational instability only when the delay is large. This will be shown in a rigorous way in the next section.

The modulational-type instability is associated with long-wavelength oscillations, since it occurs at the small frequencies $k2\pi/\tau$. In Fig. 3(b) there are 7 roots in the right-half plane and $k = 1, \ldots, 7$.

Fig. 3(c) demonstrates an unstable mode, possessing a pair of complex conjugate roots with large positive real parts. The orbits in the vicinity are repelled from such an ECM, exhibiting oscillations with the relaxation frequency.

Finally, in Fig. 3(d), an unstable antimode is shown, which has a real positive eigenvalue $\lambda > 0$. This implies fast non-oscillatory repelling from the ECM.

The following section is devoted to an analytical treatment of the stability of ECMs. We will show that the scenarios observed in Fig. 3 are typical for the Lang-Kobayashi system with large delay. We will characterize those ECMs that are strongly unstable (as in Fig. 3(c,d)) or weakly unstable (as in Fig. 3(b)). A particular attention will be paid to the maximum gain mode and the zero linewidth mode.

4 Stability of ECMs: analytical approach

The local stability properties of ECMs are determined by the characteristic equation for the linearization around the chosen ECM. For the LK system (1), this equation has the form

$$\begin{aligned}\chi(\Lambda) &= [\Lambda^2 + 2\eta\cos\theta(1-e^{-\Lambda\tau})\Lambda + \eta^2(1-e^{-\Lambda\tau})^2] \\ &\quad \times(\Lambda + \varepsilon(1+2S)) + 2\varepsilon S(1-2\eta\cos\theta) \\ &\quad \times[\Lambda + \eta(\cos\theta - \alpha\sin\theta)(1-e^{-\Lambda\tau})] = 0,\end{aligned} \tag{8}$$

where

$$S := \frac{J + \eta\cos\theta}{1 - 2\eta\cos\theta}.$$

(cf. [17, 19]). Our aim is now to study the stability properties of an ECM in the limit of large τ, depending on its position θ on the ellipse.

Some ideas of the following analysis can be found in [20], where general systems with large delay considered in an abstract way.

4.1 Strong instability.

First, we consider the case when an ECM possesses characteristic roots with large positive real parts $\mathrm{Re}\,\lambda > 0$, cf. Figs. 3(c,d). More precisely, we assume that $\mathrm{Re}\,\lambda$ does not vanish if $\tau \to \infty$.

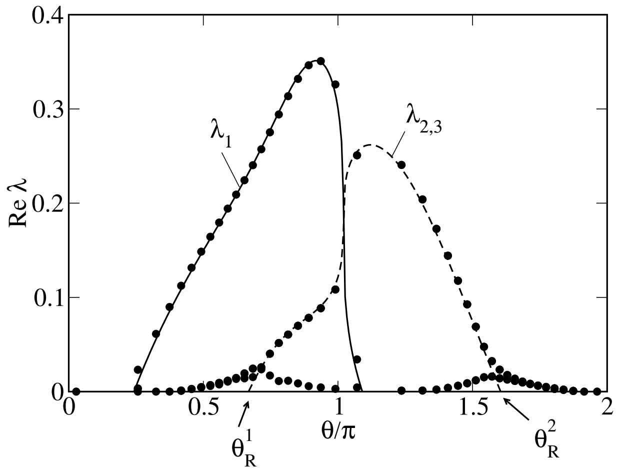

Figure 4: Maximal real parts of eigenvalues of ECMs are plotted as circles versus θ for $\tau = 100$, $\alpha = 2$, $\varepsilon = 0.03$. The lines shows analytical solutions of the approximated equation (9). Solid line denotes the real eigenvalue λ_1 and dashed line stands for the complex conjugated pair $\lambda_{2,3}$. Strongly unstable ECMs correspond to the positive λ_1 or $\lambda_{2,3}$.

In order to determine such roots, equation(8) can be simplified by neglecting terms with $e^{-\Lambda\tau}$ for sufficiently large τ. Then the approximate equation reads

$$\begin{aligned} 0 \;=\; & [\Lambda^2 + 2\Lambda\eta\cos\theta + \eta^2](\Lambda + \varepsilon(1+2S)) \\ & +2\varepsilon S(1-2\eta\cos\theta)[\Lambda + \eta(\cos\theta - \alpha\sin\theta)]. \end{aligned} \tag{9}$$

Note that (9) is a third order polynomial with respect to Λ, which was obtained from (8) by neglecting all terms containing delay. Therefore (9) is a characteristic equation of the system of equations without feedback

$$\begin{aligned} E' &= (1+i\alpha)NE, \\ N' &= \varepsilon[J - N - (2N+1)|E|^2], \end{aligned} \tag{10}$$

which has the form $\det|\Lambda I - A| = 0$, where I is the identity matrix, A is the Jacobian matrix for (10), but evaluated at the ECM of the original LK system. Note that this ECM is not a solution to (10). It is evident that such an instability is induced by the relaxation mechanism of the laser without feedback.

Although solutions of (9) are available analytically, the expressions are quite involved and we do not present them here. Instead, we plot graphs of the solutions in Fig. 4. On the same figure we plot numerically computed eigenvalues of ECMs for $\tau = 100$. The figure demonstrates good agreement. Recall that only for $\mathrm{Re}\,\lambda > 0$ the solutions of (9) are a valid approximation of the full problem.

As expected, the antimodes, i.e. $\theta_s^1 < \theta < \theta_s^2$ have a real positive eigenvalue. Additionally, ECMs with $\theta_R^1 < \theta < \theta_R^2$ have a complex conjugated pair of roots with positive real

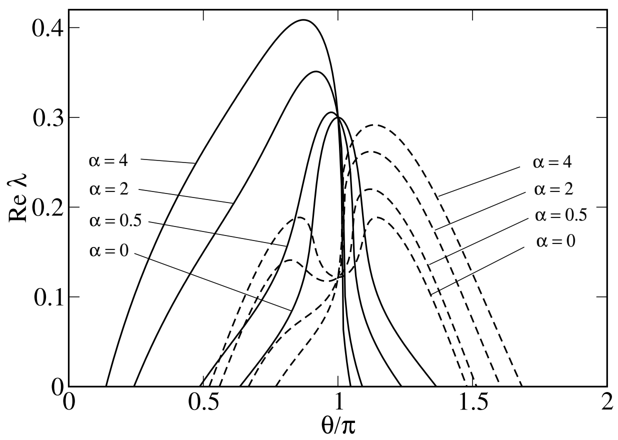

Figure 5: Influence of α-factor on the most unstable eigenvalues. Dependence of $\operatorname{Re}\lambda$ on θ.

parts. Estimates for θ_R^1 and θ_R^2 can be obtained by substituting $\Lambda = \pm i\omega$ into (9). Then, additionally taking into account smallness of ε, we obtain that up to the first order in ε

$$\theta_R^1 = \frac{\pi}{2} + \varepsilon\frac{J\alpha}{\eta^2}, \quad \theta_R^2 = -\frac{\pi}{2} + \varepsilon\frac{J\alpha}{\eta^2}.$$

Hence, the modes with positive carrier excess density N are strongly unstable possessing a pair of complex eigenvalues with positive real part and relaxation frequency.

In Fig. 5 we inspect the influence of α-factor on the strongly unstable ECMs.

One can observe that for $\alpha = 0$ the ECM with the minimal gain, i.e. $\theta = \pi$, possesses the maximal real unstable eigenvalue. The graphs for $\alpha = 0$ are symmetric with respect to the point $\theta = \pi$. With increasing α, the modes are destabilized due to the mode mixing. This is quantitatively observed in Fig. 5: the region of relaxation-oscillation instability is shifted clockwise along the ellipse, whereas the region of antimode-instability is shifted counter-clockwise. Hence the overall region of instability is growing.

Concerning the influence of the parameter ε on the strong instability, we note that with decreasing ε the solutions of (9) are tending to the following first order approximations: $\lambda_1 = 0$ and $\lambda_{2,3} = -\eta(\cos\theta + i|\sin\theta|)$. An example with $\varepsilon = 0.005$ is shown in Fig. 6.

4.2 Weak instability

In this section we consider analytically another type of instability, shown in Fig. 3(b). Numerical observations indicate that the unstable eigenvalues in this case tend to zero as τ increases (otherwise we obtain the situation considered in the previous section, cf. [20]). Consequently, now the term $e^{-\Lambda\tau}$ in (8) is large compared to the terms Λ^n, $n =$

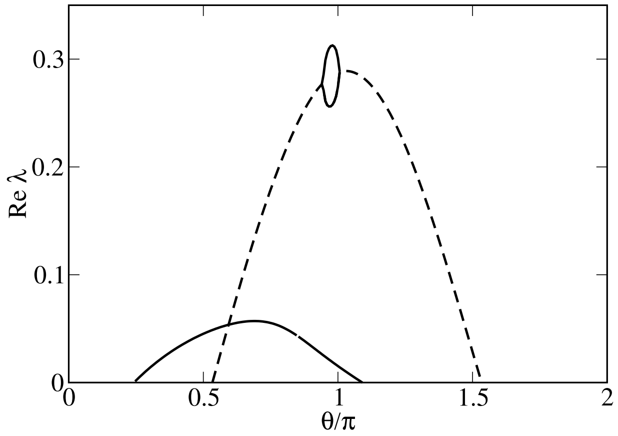

Figure 6: $\mathrm{Re}\,\lambda$ versus θ for $\varepsilon = 0.005$

1, 2, 3. Neglecting these smaller terms, we obtain the following approximate characteristic equation:

$$\begin{aligned} 0 &= (1 - e^{-\Lambda\tau})\big[\eta(1+2S)(1-e^{-\Lambda\tau}) \\ &\quad +2S(1-2\eta\cos\theta)(\cos\theta - \alpha\sin\theta)\big]. \end{aligned} \tag{11}$$

Equation (11) defines two infinite branches of eigenvalues

$$\lambda_{\mathrm{c}} = i\frac{2\pi}{\tau}k, \tag{12}$$

$$\lambda_{\mathrm{n}} = \frac{\mathrm{Ln}\ \mu(\theta)}{\tau} + i\frac{2\pi}{\tau}k, \tag{13}$$

where k is any integer number, which can be considered as a parameter along the branches,

$$\mu(\theta) = \left[1 + \frac{2S(1-2\eta\cos\theta)(\cos\theta - \alpha\sin\theta)}{\eta(1+2S)}\right]^{-1},$$

and $\mathrm{Ln}\ \mu(\theta) = \ln|\mu(\theta)| + i\mathrm{A}rg\ \mu(\theta)$.

Expressions (12) and (13) give asymptotic values for two branches of eigenvalues. These branches can be already seen in Fig. 3. As $\tau \to \infty$, in a vicinity of the origin both branches asymptotically tend to the imaginary axis and their number in this vicinity increases. Therefore, for large τ all ECMs possess a large number of eigenvalues, which are close to the imaginary axis (note the scaling in Fig. 3).

Let us clarify the origin of these branches. Recall that Eq. (11) was obtained from the characteristic equation (8) of the LK system by neglecting terms proportional to Λ^n. Since these terms appear due to the temporal derivatives, the simplified Eq. (11) corresponds to

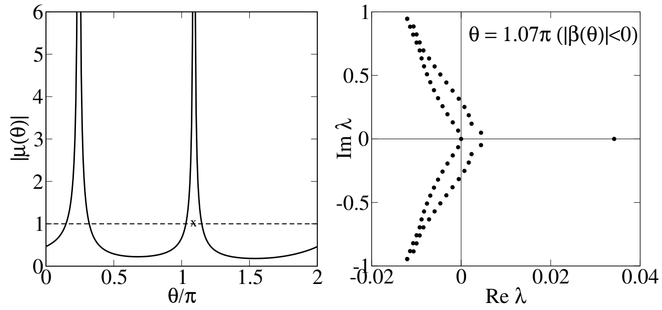

Figure 7: For $|\mu(\theta)| > 1$, the noncritical branch of characteristic roots is partially located at $\mathrm{Re}\,\lambda > 0$. (a): Dependence of $|\mu(\theta)|$; (b): characteristic roots for the case $\theta = 1.07$, $\tau = 100$, $\varphi = 1.0$, $\varepsilon = 0.03$, $J = 1$.

the mapping, which is implicitly given by

$$\begin{aligned} 0 &= (1 + i\alpha)N(t)E(t) + \eta e^{-i\varphi}E(t - \tau), \\ 0 &= \varepsilon[J - N(t) - (2N(t) + 1)|E(t)|^2]. \end{aligned} \tag{14}$$

Therefore, the mapping (14) is responsible for the formation of these branches of eigenvalues of ECMs. In particular, one can check that $\mu(\theta)$ and 1 are the multipliers of (14), computed at the corresponding ECM solution.

On a more intuitive level, one can explain it in the following way: when the delay is large, the feedback term can play an important role only for those eigenmodes of ECM, which are either stable or weakly unstable with the growth slower then e^{at}, where $a \sim \frac{1}{\tau}$. In this case the influence of the feedback is essential $|E(t-\tau)/E(t)| = e^{-a\tau} \sim 1$.

Having realized the origin of the branches of eigenvalues in Fig. 3, we now discuss how they can induce instabilities. The first possibility for instability is the case when the mapping (14) is unstable, i.e. $|\mu(\theta)| > 1$. Then noncritical branch (13) contains unstable roots. For a specific choice of parameters, the behavior of $|\mu(\theta)|$ and the corresponding configuration of eigenvalues are shown in Fig. 7. Note that there is an additional positive real eigenvalue. Hence, we claim that this type of instability does not play an important role in the LK system, since it coexists with the strong instability, at least for the range of parameter values considered here.

The instability of modes caused by the critical branch, cf. Fig. 3(b) seems to be of more importance. The first order approximation of the critical branch, given by (12) is not sufficient to describe its curvature. Therefore, we find the next terms in the approximation by inserting

$$\Lambda = i\frac{2\pi}{\tau}k + \frac{1}{\tau^2}\lambda_1 + \frac{1}{\tau^3}\lambda_2 + \cdots$$

into the original characteristic equation (8). By standard perturbation technique, we obtain

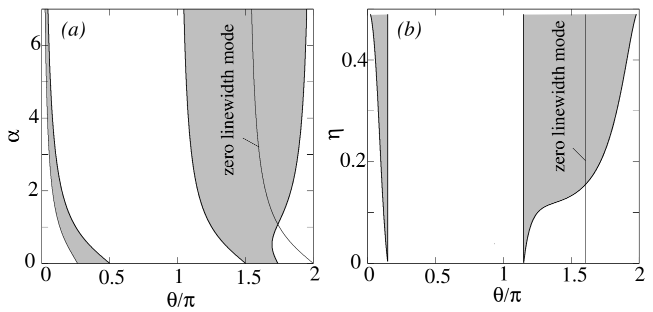

Figure 8: Parameter values, corresponding to modulational instability are shown in gray. They correspond to the case when the critical branch of characteristic roots have positive curvature $\mathrm{Re}\,\lambda_2 > 0$, similarly to Fig. 3(b). Parameter values: $\eta = 0.3$ for Fig. (a) and $\alpha = 2$, for Fig. (b). For the both figures $J = 1$.

the following expressions for λ_1 and λ_2:

$$\lambda_1 = -i\frac{2\pi k}{\eta(\cos\theta - \alpha\sin\theta)}, \tag{15}$$

$$\begin{aligned}\lambda_2 = & \frac{(1+2S)(4\pi^2k^2 - i4\pi k\eta\cos\theta\lambda_1 - \eta^2\lambda_1^2)}{2\eta(J+\eta\cos\theta)(\cos\theta - \alpha\sin\theta)} \\ & -\frac{\lambda_1}{\eta(\cos\theta - \alpha\sin\theta)} - \frac{1}{2}\lambda_1^2.\end{aligned} \tag{16}$$

It is easy to see that $\mathrm{Re}\,\lambda_1 = 0$ and $\mathrm{Re}\,\lambda_2 \neq 0$. Moreover, $\mathrm{Re}\,\lambda_2$ is proportional to k^2. Therefore, we conclude that the critical branch is generally tangent to the imaginary axis at the origin. The sign of $\mathrm{Re}\,\lambda_2$ determines the curvature at the origin of the critical branch, for example, $\mathrm{Re}\,\lambda_2 < 0$ in Fig. 3(a) and $\mathrm{Re}\,\lambda_2 > 0$ in Fig. 3(b).

The case with $\mathrm{Re}\,\lambda_2 > 0$ can be considered as a criterion for modulational instability of the delay system. It can be studied with respect to different parameters. The examples of such results are shown in Fig. 8. The figure shows, that with increasing α, as well as with increasing of the feedback strength η, a larger number of modes become involved in this type of instability. In particular, there is a threshold $\alpha_{\max}$ and $\eta_{\max}$ for the zero-linewidth mode after which at $\alpha > \alpha_{\max}$ or $\eta > \eta_{\max}$ this ECM is unstable.

5 Classification of ECMs accordingly to their stability properties

As we have shown in the previous section, the particular cases of eigenvalues configuration of ECMs shown in Figs. 3 are typical for the Lang-Kobayashi system (1) with large delay. Section 4 contains analytic formulas, which help to determine which instability takes place for a given ECM. Here we shortly summarize:

- *Antimode instability.* ECMs with $\theta_s^1 < \theta < \theta_s^2$ have real positive eigenvalue, cf. Fig. 3(d).

- *Relaxation strong instability.* The modes with $\theta_R^1 < \theta < \theta_R^2$ have an unstable pair of complex-conjugated eigenvalues with the relaxation oscillation frequency, cf. Fig. 3(c).

- *Modulational instability.* The modes, which are not strongly stable can display a weak modulational instability, cf. Fig. 3(b). Fig. 8 shows that such type of instability is common for many ECMs, including those, which are close to the maximum gain mode and zero linewidth mode. Therefore one might assume, that this is a common feature for ECMs that form a skeleton of chaotic low-frequency fluctuations in LK system [13]. It is shown that increasing α and η acts in favor of such type of instability. Such ECMs become highly degenerate with increasing delay, i.e. they possess a large number of eigenvalues with very small (and positive) real parts.

- *Stable modes.* For some parameter values, asymptotically stable ECMs appear, as shown in Fig. 3(a). Our analysis shows that such modes are more probable to appear with decreasing α or η. The leading stable direction of such ECMs corresponds to the pair of complex characteristic roots $\pm i2\pi/\tau$.

Let us consider separately two cases.

Case 1: Maximum gain mode. The inspection of (8) shows that stability properties of the maximum gain mode ($\theta = 0$) does not depend on the α-factor. This means, in particular, that increasing α does not destabilize the maximum gain mode. Our numerical study in Fig. 9 shows that with changing η this mode remains stable. This observation is in favor of the hypothesis, that a stable ECM coexists with the chaotic attractors of LK system for a large parameter range, including arbitrary large delays.

Case 2: Zero linewidth mode. This mode is proved to become unstable as α or η increase. After the destabilization, it exhibits a modulational type instability. Taking into account the probability distribution of modes, cf. Sec. 2, it is the most probable mode in LK system.

6 ECMs and chaotic pulsations

The main result of the present paper is supposed to give an additional insight into the properties of ECMs of the feedback system (1). We believe that they can lead to a deeper understanding of the complex behavior of the solutions of the Lang-Kobayashi model with large feedback time and, in particular, into the nature of so called low-frequency fluctuations.

It is widely accepted that low-periodic orbits form a ßkeletonöf a chaotic attractor [2, 7, 11, 18]. Concerning the LK model, the traditional point of view was to consider ECMs as the skeleton for low-frequency fluctuations. Recently it was suggested in [4] that the

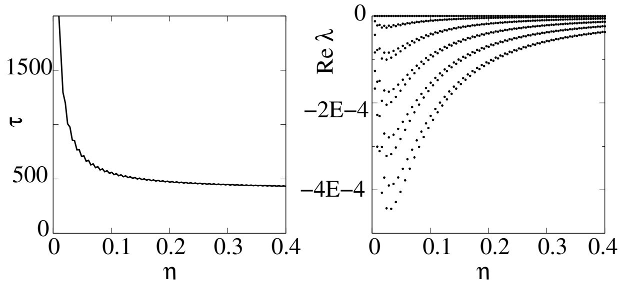

Figure 9: The right figure shows behavior of the leading characteristic roots of the maximum gain mode with $\theta = 0$. The left figure shows dependence of τ on η for the calculated solutions. This dependence guarantees the existence of the mode with $\theta = 0$, cf. (5).

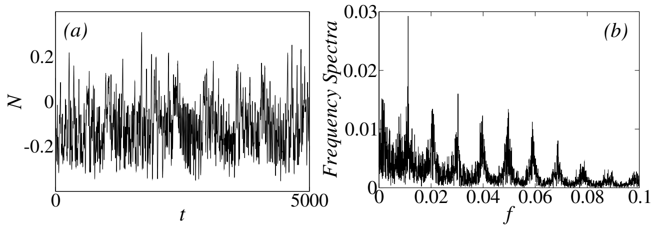

Figure 10: (a) Chaotic orbit of Lang-Kobayashi system for $\alpha = 5$, $J = 1$, $\varepsilon = 0.03$, $\eta = 0.3$, and $\varphi = 0$. (b) Power spectrum of the signal.

proper candidates for such elementary orbits in LK system are other regular attractors, which are created via bifurcations of ECMs. To support this point of view, we note that the periodic orbits of chaotic systems without additional symmetries rather correspond to the modulated wave solutions [19] of LK system, which are tori in the phase space. Such a difference is caused by the rotational symmetry of LK model.

Even though ECMs are not forming the skeleton of the chaotic attractor in LK system, the study of their stability do not become less important. One of the arguments in the favor of the importance of ECMs is the following: Since the regular attractors eventually bifurcate from ECMs and are located close to them, they inherit many properties of ECMs, including the number and types of leading directions, etc. In this case properties of this attractors can be deduced from the properties of ECMs.

Let us consider two examples. Fig. 10 shows a chaotic orbit of (1). The power spectrum of the orbit clearly demonstrates peaks at the frequencies k/τ, where $k = 1, 2, \dots$. This known fact can now be explained in terms of ECMs. Namely, when the orbit is close to some ECM, then mainly the leading eigenvalues influence this orbit. Since the leading directions of ECMs are characterized by the frequencies k/τ (cf. Sec. 4), they are also seen in the spectra of the chaotic signal.

Another example in Fig. 11 shows the dependence of the maximal Lyapunov exponents on the delay parameter. We can observe, that their amplitude decreases, making the attractor degenerate in the sense that many Lyapunov exponents eventually tend to zero. This fact

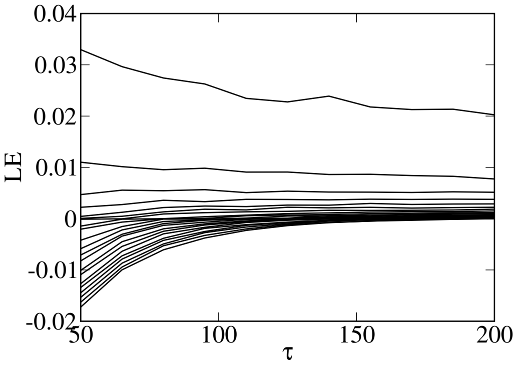

Figure 11: Maximal Lyapunov exponents of the attractor of LK model versus τ. Other parameters are $\alpha = 5$, $J = 1$, $\varepsilon = 0.03$.

is consistent with the asymptotic behavior of the critical characteristic roots of weekly stable ECMs.

This work was supported by DFG (Sonderforschungsbereich 555 “Komplexe nichtlineare Prozesse“).

References

[1] P. M. Alsing, V. Kovanis, A. Gavrielides, and T. Erneux. Lang and kobayashi phase equation. *Phys. Rev. A*, 53:4429–4434, 1996.

[2] D. Auerbach, P. Cvitanović, J.-P. Eckmann, G. Gunaratne, and I. Procaccia. *Phys. Rev. Lett.*, 58:2387, 1987.

[3] Ruslan L. Davidchack, Ying-Cheng Lai, Athanasios Gavrielides, and Vassilios Kovanis. Chaotic transitions and low-frequency fluctuations in semiconductor lasers with optical feedback. *Physica D*, 145:130–143, 2000.

[4] Ruslan L. Davidchack, Ying-Cheng Lai, Athanasios Gavrielides, and Vassilios Kovanis. Regular dynamics of low-frequency fluctuations in external cavity semiconductor lasers. *Phys. Rev. E*, 63:056206, 2001.

[5] K. Engelborghs, T. Luzyanina, and G. Samaey. DDE-BIFTOOL v. 2.00: a Matlab package for bifurcation analysis of delay differential equations. Technical Report TW-330, Department of Computer Science, K.U.Leuven, Leuven, Belgium, 2001.

[6] G. Giacomelli and A. Politi. Relationship between delayed and spatially extended dynamical systems. *Phys. Rev. Lett.*, 76(15):2686–2689, 1996.

[7] C. Grebogi, E. Ott, and J. A. Yorke. *Phys. Rev. A*, 37:1711, 1988.

[8] T. Heil, I. Fischer, W. Elsäßer, and A. Gavrielides. Lang and kobayashi phase equationdynamics of semiconductor lasers subject to delayed optical feedback: The short cavity regime. *Phys. Rev. Lett.*, 87:243901, 2001.

[9] J. Javaloyes, Paul Mandel, and D. Pieroux. Dynamical properties of lasers coupled face to face. *Phys. Rev. E*, 67:036201, 2003.

[10] I. V. Koryukin and Paul Mandel. Two regimes of synchronization in unidirectionally coupled semiconductor lasers. *Phys. Rev. E*, 65:026201, 2002.

[11] Y.-C. Lai, Y. Nagai, and C. Grebogi. *Phys. Rev. Lett.*, 79:649, 1997.

[12] R. Lang and K. Kobayashi. *IEEE J. Quantum Electron.*, 16:347, 1980.

[13] Jesper Mørk, Bjarne Tromborg, and Jannik Mark. Chaos in semiconductor lasers with optical feedback: theory and experimet. *IEEE J. Quantum Electron.*, 28:93–108, 1992.

[14] Michael Peil, Tilmann Heil, Ingo Fischer, and Wolfgang Elsäßer. Synchronization of chaotic semiconductor laser systems: a vectorial coupling-dependent scenario. *Phys. Rev. Lett.*, 88:174101, 2002.

[15] M. Tlidi, A. G. Vladimirov, and Paul Mandel. Curvature instability in passive diffractive resonators. *Phys. Rev. Lett.*, 89(23):233901, 2002.

[16] G. H. M. van Tartwijk and G. P. Agarwal. *Prog. Quantum Electron.*, 22:43, 1998.

[17] Matthias Wolfrum and Dmitry Turaev. Instabilities of lasers with moderately delayed optical feedback. *Opt. Commun.*, 212:127–138, 2002.

[18] S. Yanchuk and T. Kapitaniak. Chaos-hyperchaos transition in coupled rössle systems. 290:139, 2001.

[19] S. Yanchuk, K. R. Schneider, and L. Recke. Dynamics of two mutually coupled semiconductor lasers: Instantaneous coupling limit. *Phys. Rev. E*, 69:056221, 2004.

[20] Serhiy Yanchuk. Properties of stationary states of delay equations with large delay and applications to laser dynamics. *Math. Meth. Appl. Sci.*, to appear.